Article

Not peer-reviewed version

Experimental and Clinical Study of Flap Monitoring with Analysis of Clinical Course of the Flap Using Infrared Thermal Camera

Hyun Kim , Si Hyun Kwak , Je Yeon Byeon , Da Woon Lee , Jun Hyuk Kim , Soomin Lim , Hwan Jun Choi *

Posted Date: 18 June 2024

doi: 10.20944/preprints202406.1185.v1

Keywords: Free tissue flaps; Surgical flaps; Differential thermal analysis

 doi:10.20944/preprints202406.1185.v1

Article

Experimental and Clinical Study of Flap Monitoring with Analysis of Clinical Course of the Flap Using Infrared Thermal Camera

Hyun Kim [1], Si Hyun Kwak [1], Je Yeon Byeon [1], Da Woon Lee [1], Jun Hyuk Kim [1], Soomin Lim [2] and Hwan Jun Choi [1,*]

[1] Department of Plastic and Reconstructive Surgery, Soonchunhyang University Cheonan Hospital, Cheonan, South Korea.
[2] Bachelor of Medicine and Bachelor of Surgery(MBBS), UCL Medical School, University College London, London, UK
* Correspondence: Soonchunhyang University Cheonan Hospital, 31 Suncheonhyang 6-gil, Dongnam-gu, Cheonan 31151, Korea, iprskorea@gmail.com; Tel.: +82-41-574-6133

Abstract: Flap surgery is a common method used to cover defects following tumor ablation, trauma, or infection. However, insufficient vascularity in the transferred flap can lead to flap necrosis and failure. Proper postoperative monitoring is essential to prevent these complications. Recently, research has explored the use of infrared thermal imaging in plastic surgery, leading to its clinical application. This study investigates the use of a forward-looking infrared (FLIR) camera to monitor blood flow in flaps. In the study, 28 rats underwent reverse McFarlane flap surgery, and their flaps were analyzed using a FLIR thermal imaging camera seven days post-surgery. Additionally, thermal images of flaps were taken on postoperative days 0, 1, 2, 3, and 7 in 22 patients. The study focused on temperature differences between normal skin and the perforator compared to the average flap temperature. Results showed that the temperature difference was higher in the necrosis group and increased over time in cases of total necrosis. A lower perforator temperature compared to the flap's average indicated vascular compromise, potentially leading to flap failure. The FLIR camera, being contact-free and convenient, shows promise for understanding and inferring the clinical progression of flaps in postoperative monitoring.

Keywords: free tissue flaps; surgical flaps; differential thermal analysis

1. Introduction

Flap surgery is a technique in plastic and reconstructive surgery where any type of tissue is lifted from a donor site and moved to a recipient site with intact blood supply. This is done to fill a defect such as a wound as a consequence of injuries or surgery, when the remaining tissue is unable to support a graft, or to rebuild more complex anatomic structures such as the breast or jaw. It stands as a cornerstone of reconstructive procedures, playing a pivotal role in the restoration of form and function following trauma, oncologic resection, or congenital malformation [1]. The success rate of flap surgery relies on meticulous surgical technique and postoperative monitoring to assess tissue viability and mitigate complications [2].

Post-operative monitoring of free flaps is important in flap survival, immediate action increases flap salvage rate. Although various methods are available, room for improvement remains. Currently, free flap monitoring can be done through a variety of methods, including physical examination (skin color, turgor, temperature, and capillary refill), surface temperature recording, external doppler, implantable doppler, color duplex sonography, laser doppler flowmetry, infrared thermography, near-infrared spectroscopy, white light spectroscopy, and microdialysis. Despite the extensive exploration of monitoring methodologies, the absence of a definitive gold standard persists, which necessitates continued investigation into novel approaches [3,4].

Thermal cameras have proven their value in medicine and are nowadays readily available at a low cost. Their non-invasive nature and ability to provide immediate, quantitative data make infrared thermal imaging an attractive adjunct in flap monitoring [5]. Various clinical applications

 doi:10.20944/preprints202406.1185.v1

involving depth analysis of burns, detection of complications for diabetic foot ulcer and preoperative planning of perforators using infrared thermal imaging have been made in plastic surgery [6,7]. Furthermore, there have been several publications describing flap monitoring using infrared thermal imaging [5].

This study aims to present a new perspective on the clinical course of flaps in flap monitoring by taking advantage of the convenience of forward-looking infrared (FLIR) thermal cameras, focusing on the correlation between flap necrosis and temperature comparison of flaps from a different thermal analysis perspective than previous studies.

2. Materials and Methods

2.1. Rat Models

The *in vivo* experimental protocols and study were approved by the Institutional Animal Care and Use Committee (IACUC) of Soonchunhyang University (Approval number: SCH-0062). In total, 28 transgenic Spraque-Dawley (SD) rats (12 weeks) were involved in this study. On the day of implantation, all rats were trimmed over the backside under anesthesia with isoflurane (Terrel, USA), oxygen and N_2O. In this study, a reverse McFarlane skin flap of 3×9 ㎝ size was elevated using a blade to induce skin necrosis models to evaluate skin flaps. The flap was immediately closed by suturing with 4-0 nylon (AILEE Co., Korea) (Figure 1). The entire area was covered by gauze and then appropriately bandaged without disturbing the gauze over the wounds. To relieve their pain and prevent infection, tramadol and enrofloxacin were given intramuscularly. All rats were individually isolated in each cage at controlled temperatures (25℃) and sacrificed on the planned time points (Day 7). The experimental photographs were taken using a Cannon EOS R6 Mark Ⅱ (Tokyo, Japan) camera at a standard distance (40 ㎝) to assess the wounds and flaps on postoperative day (POD) 3 and POD 7. The thermal images were obtained by FLIR camera on POD 3 and POD 7. We calculated the ratio of necroitc area/total area and analyzed the difference between necrotic area and non-necrotic area using Fiji-ImageJ software(ImageJ, US).

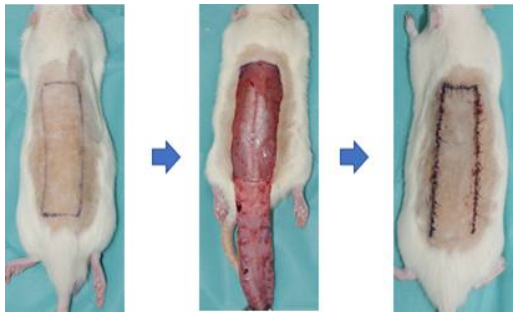

Figure 1. Schematic diagram of surgical procedures. Incisions were made on the back of the mouse under anesthesia with isoflurane, and a 3x9cm sized reverse McFarlane skin flap was elevated using a blade. The flap was immediately closed with sutures using 4-0 nylon.

2.2. Patients

The protocol of this study was approved by the Institutional Review Board approval (IRB number: 2023-12-071) Patients who underwent pedicled flap or free flap surgery on any locations of the body between December 2021 and September 2023 were included. Patients with distinct hypothermia or hyperthermia were excluded. Also, the buried flaps were excluded. All patients were advised to take absolute bed rest for a week and given intravenous antibiotics for preoperative and postoperative infection control. The clinical photographs were taken using an ILCE-7M4 (Sony®, Tokyo, Japan) camera at a standard distance (40 ㎝) to assess the wounds and flaps.

2.3. Infrared Thermal Imaging

Thermal images were captured using the FLIR C5 camera (Teledyne FLIR LLC, US). The FLIR C5 has two cameras a thermal imager (160×120 pixels) and 5-megapixel visual camera (640×480 pixel), and LED flashlight. Two images were obtained and merged by the Multi Spectral Dynamic Imaging

 doi:10.20944/preprints202406.1185.v1

(MSX) technology, resulting in one thermal image with resolution of 640×480 pixels. It has the capacity of detect temperature ranging of -20°C to 400°C and the thermal sensitivity is <70mK.

All flaps were monitored at POD 0, 1, 2, 3 & 7, and some flaps even up to 2 weeks with FLIR camera and clinical findings such as skin color and capillary refill time. The thermal imaging was performed at operating room with a controlled temperature (18-22°C) and humidity (50-55%). To reduce the temperature bias, thermal imaging was performed 10 minutes after the patient entered the operating room. The images were captured at a distance of 40 ㎝ from the flaps. After monitoring, the dressing methods for all flaps were equally controlled with the use of ointments and gauze. If the location of the flap was in an area where splinting was possible, the instability of the flap was reduced through the use of a splint.

2.4. Infrared Thermal Image Analysis

The authors also used the FLIR Thermal Studio software (Teledyne FLIR LLC, US) to analyze the thermal images which allows to identify the temperature of a specific point or area on a thermal image and calculate the temperature difference (Figure 2).

On the obtained thermal images, the authors marked the range of the total flap area and measured the average of temperature value of the flap area (ATF) at imaging software program. In addition, we measured the temperature of the perforator of the flap (PF), as well as the normal skin (NS) at the point 2cm proximal from the flap in anatomical position. The temperature difference (dT) between normal skin and the perforator of the flap was compared. In addition, the temperature difference of the perforator and the average temperature of flap (AFP) was obtained.

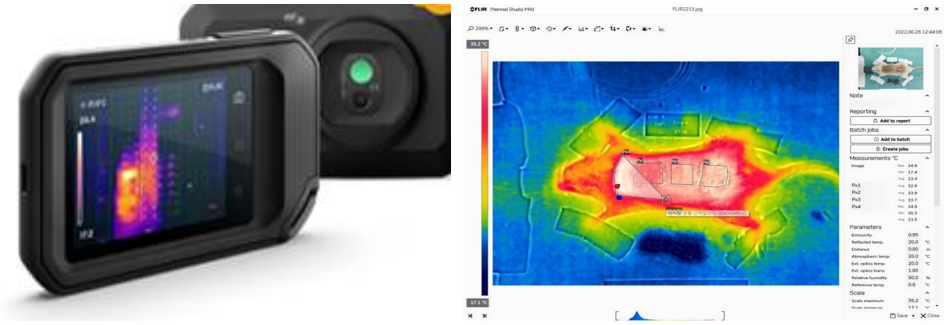

(**a**) (**b**)

Figure 2. FLIR camera & Thermal analysis software. (**a**) The FLIR C5 camera (Teledyne FLIR LLC, US) has two cameras - A thermal imager (160x120 pixels) and 5-megapixel visual camera (640x480 pixel). (**b**) FLIR Thermal Studio software (Teledyne FLIR LLC, US) is displayed on the right – Used to analyze the thermal images, which allows the user to identify the temperature of a specific point or area on the image and calculate the temperature difference.

2.5. Statistical Analysis

Statistical significance was determined using the Mann-Whitney u test for independent groups. All statistical analyses were performed using SPSS (ver 27; IBM Corp., Armonk, NY, USA). A *p*-value of less than 0.05 was considered statistically significant.

3. Results

3.1. Rat Models

The degree of necrosis of the flaps was evaluated by flap color and skin turgor on POD 3 and POD 7. The necrotic part of the flap was dark in color and appeared to dry out hard. On POD 7, all rats were euthanized, and sutures were removed to evaluate the undersurface of the flap, and the difference in necrosis of the flap was more noticeable on the undersurface of the flap. The mean surface area of total flap was 27.12±0.90 ㎠, and mean ratio of total flap area over the necrotic area were 24.4% and 27.5% in POD 3 and POD7 respectively. On thermal imaging, the necrotic flap was clearly distinguished from the viable flap by color differences, with areas of high temperature being

 doi:10.20944/preprints202406.1185.v1

white and areas of low temperatures being red (Figure 3). The mean temperature difference in each area was 0.8℃ in POD 3 and 0.792℃ in POD 7 (Table 1).

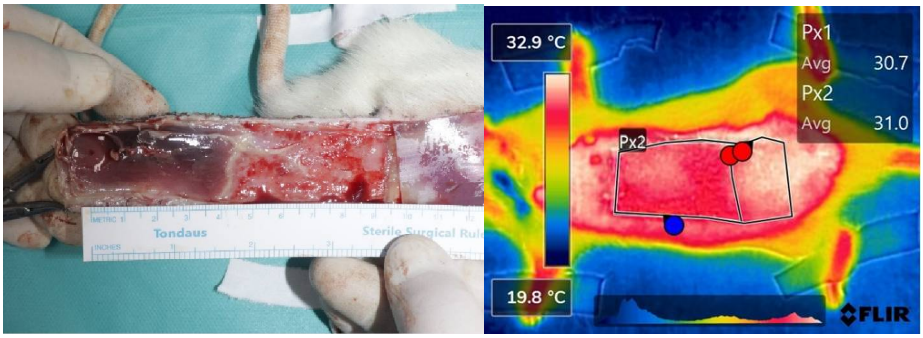

(**a**) (**b**)

Figure 3. Analysis of flap necrosis in rat models. (**a**) After euthanization of the rats, the total flap and necrotic area was measured with distinguishment of flap viability. (**b**) The thermal images were captured by FLIR camera indicating the necrosis area (colored red), which shows a drop in temperature compared to the viable area (colored white). The temperature difference between the total flap area and necrotic area was calculated by using infrared thermal software.

Table 1. Thermal analysis of rat models.

Flap models (n=28)	POD 3	POD 7
Necrotic area/Total flap ratio (%)	24.4	27.5
Temperature difference between total flap and necrotic area	0.800	0.792

Abbreviations : POD, postoperative day

3.2. Patients

3.2.1. Patient Demographics & Flap Characteristics

In total, 22 patients and 22 flaps were included in this study. There was a total of 16 male and 6 female patients, with a total average age of 57.45 years (range: 27 to 100). All flaps were either pedicled flaps (14 in total) or free flaps (8 in total). Various pedicled flaps were made depending on the location of the defect and the surrounding vascularity and an anterolateral thigh (ALT) free flap was used for free flap reconstruction in all cases except 2. Necrosis occurred in 2 cases of the free flap group due to arterial insufficiency, and 1 case of total necrosis occurred in the free flap group due to venous congestion. In the pedicled flap group, 1 case of partial necrosis occurred. Initially, arterial insufficiency occurred in 3 cases, but despite salvage procedures being performed in 2 of these cases, flap failure occurred, and a new flap was reapplied. One of these cases survived stably without necrosis, so it was not included in the necrosis group. The location of the flap site varied from the scalp to the lower extremity. There was no other complication such as hematoma or infection (Table 2, Table 3).

Table 2. Patients demographics.

No. of patient	Sex	Age	Location	Flap	Flap type	Flap necrosis
1	M	61	Lt. ankle	ALT free flap	Free flap	No necrosis
2	F	27	Scalp	ALT free flap	Free flap	No necrosis
3	M	16	Lt. ankle	ALT free flap	Free flap	No necrosis
4	M	55	Lt. lower leg	ALT free flap	Free flap	No necrosis
5	M	72	Philtrum	ALT free flap	Free flap	No necrosis
6	F	66	Lt. ankle	ALT free flap	Free flap	No necrosis

 doi:10.20944/preprints202406.1185.v1

7	F	100	Lt. upper eyelid	ALT free flap	Free flap	No necrosis
8	M	60	Lt. foot	ALT free flap	Free flap	Total necrosis
9	M	63	Lt. ankle	ALT free flap	Free flap	No necrosis
10	M	51	Lt. foot	ALT free flap	Free flap	Total necrosis
11	F	70	Rt. foot	ALT free flap	Free flap	No necrosis
12	M	48	Lt. ankle	TDAP free flap → ALT free flap	Free flap	No necrosis
13	F	23	Lt. hand	SCIP free flap	Free flap	No necrosis
14	M	75	Scalp	ALT free flap → Vastus lateralis muscle free flap	Free flap	Total necrosis
15	M	81	Nose	Nasolabial fold flap	Pedicled flap	No necrosis
16	M	56	Nose	Nasolabial fold flap	Pedicled flap	No necrosis
17	M	52	Nose	Nasolabial fold flap	Pedicled flap	No necrosis
18	M	91	Nose	Paramedian forehead flap	Pedicled flap	No necrosis
19	M	57	Nose	Paramedian forehead flap	Pedicled flap	No necrosis
20	M	57	Rt. lower leg	ALT pedicled flap	Pedicled flap	No necrosis
21	F	49	Rt. ankle	Peroneal artery perforator based FC rotation flap	Pedicled flap	Partial necrosis

Abbreviations: Rt, right; Lt, left; ALT, The anterolateral thigh; TDAP, The thoracodorsal artery perforator; SCIP, The superficial circumflex iliac artery perforator; FC, fasciocutaneous.

Table 3. Flap charactertistics.

	Necrosis goupe (n=4)
Necrosis type	
Total necrosis	3
Partial necrosis	1
Vascular compromise	
Arterial insufficiency	2
Venous congestion	2

3.2.2. Infrared Thermal Imaging Analysis

The temperature difference between normal skin and the perforator (dT of NS-PF) in the non-necrosis group showed a gradual decrease over time, while that in necrosis group increased.

In POD 0, the temperature difference between normal skin and perforator (dT of NS-PF) was shown to be lower in the necrosis group (1.55) than in the non-necrosis group (1.817). However, from POD 1 to 7, the Necrosis group showed higher dT of NS-PF values than the non-necrosis group. Among them, there was a statistically significant difference between the non-necrosis group and the necrosis group in POD 3 and POD 7. When the necrosis group was subdivided, the difference between the total necrosis group and the non-necrosis group became higher.

The difference between the perforator temperature and the average temperature of the flap (dT of PF-AFP) showed positive values from POD 0 to POD 7 in the non-necrosis group, while the necrosis group showed negative values from POD 1 to POD 7. On POD 1, the dT of PF-AFP was significantly different between the non-necrosis group (0.35) and the necrosis group (-0.175) with a p-value of 0.002. This trend continued with significant differences on POD 2 ($p = 0.003$), POD 3 ($p < 0.001$), and POD 7 ($p < 0.001$)(Table 4).

Table 4. Analysis of comparison between non-necrosis group and necrosis group.

 doi:10.20944/preprints202406.1185.v1

	Non necrosis (n=18)	Necrosis (n=4)		
			Total necrosis (n=3)	Partial necrosis (n=1)
Age (yrs)	57.167	58.75		
Sex				
Male	13	3		
Female	5	1		
Temperature difference (dT) of Normal skin – Perforator (NS-PF) (℃)				
POD 0	1.817	1.55 (0.484)	1.633 (0.740)	1.3 (0.526)
POD 1	1.533	1.875 (0.434)	2 (0.262)	1.5 (0.842)
POD 2	1.528	2.2 (0.434)	2.467 (0.262)	1.4 (0.842)
POD 3	0.989	2.525 (0.001*)	2.533 (0.006*)	2.5 (0.105)
POD 7	0.706	3.5 (<0.001*)	4 (0.002*)	2 (0.105)
Temperature difference (dT) of Perforator – Average of flap (PF-AFP) (℃)				
POD 0	0.539	0.175 (0.118)	0.2	0.1
POD 1	0.35	-0.175 (0.002*)	-0.2	-0.1
POD 2	0.333	-0.225 (0.003*)	-0.2	-0.3
POD 3	0.617	-0.375 (<0.001*)	-0.233	-0.8
POD 7	0.489	-0.225 (<0.001*)	-0.333	-0.1

Note: Values are expressed as mean. The value between the parentheses corresponds to the p-value for statistical significance between the group and the non-necrosis group. *p-value < 0.05. Abbreviations: POD - Post-Operative Day; dT - Temperature Difference; NS-PF - normal skin-perforator; PF-AFP - perforator-average of flap.

3.2.3. Case of Non-Necrosis Group (Case #7 & Case #13)

Case #7 is a 100-year-old female patient with no past medical history aside from squamous cell carcinoma of the left upper eyelid. She underwent reconstruction through ALT free flap after resection of the full-thickness skin including the tumor on the left upper eyelid. Case #13, a healthy 23-year-old female patient, was reconstructed through superficial circumflex iliac artery perforator (SCIP) free flap after distal finger necrosis caused by the use of vasopressors due to septic shock. Both cases showed stable progress without necrosis, and the temperature difference between normal skin and perforator (dT of NS-PF) showed a decreasing trend over time (Figure 4). On POD 0, the dT of NS-PF for Case #7 and Case #13 were 0.9 and 1.4, respectively. However, by POD 7, the dT of NS-PF had decreased to 0.4 and 0.5 for Case #7 and Case #13, respectively, indicating a reduction in temperature difference over time. This decrease in dT of NS-PF reflects the stabilization and successful integration of the flap without vascular compromise. The thermal images of both cases on POD 7 showed a similar color to the surrounding area except for some margins, indicating no signs of necrosis. Both flaps survived stably without any necrosis and the patients were discharged after POD 14.

 doi:10.20944/preprints202406.1185.v1

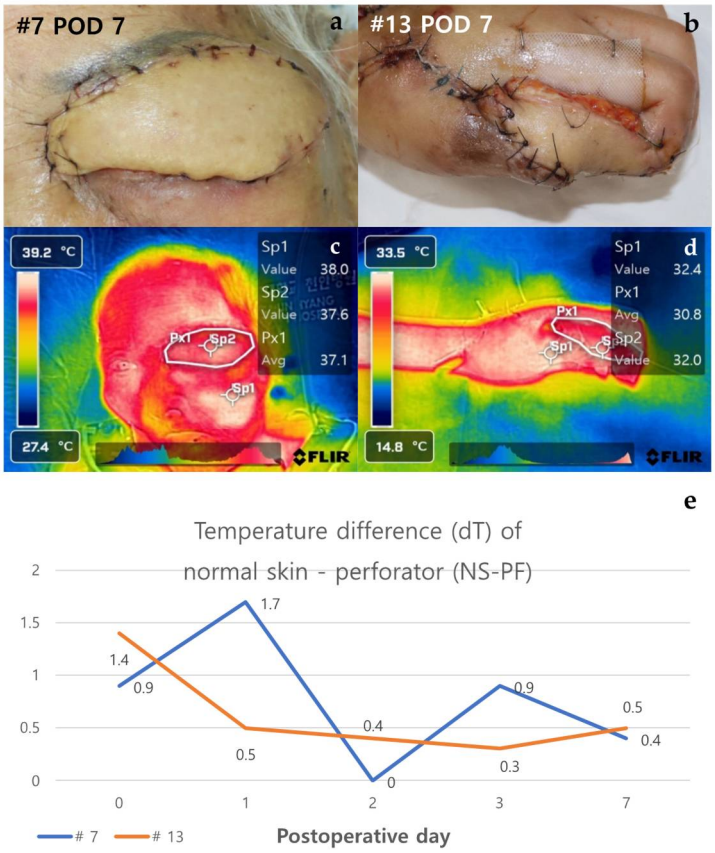

Figure 4. Analysis of cases of non-necrosis group (Case #7 & Case #13). (**a**) Case #7 - A 100-year-old female patient underwent reconstruction through ALT free flap after tumor resection due to skin cancer on the left upper eyelid. On POD 7, the flap maintained stably without any necrosis. (**b**) Case #13 - A 23-year-old female patient who underwent SCIP free flap reconstruction after distal finger necrosis due to use of vasopressors. On POD 7, the flap has no necrosis. (**c**), (**d**) In the thermal images of POD 7, both flaps have a similar color to the surrounding area except for some margins. (**e**) The graph shows NS-PF decreasing over time. Abbreviations: POD, Post-Operative Day; dT, Temperature Difference; NS-PF, normal skin-perforator; ALT free flap, The anterolateral thigh free flap; SCIP free flap, The superficial circumflex iliac artery perforator free.

3.2.4. Case of Venous Congestion in Necrosis Group (Case #10 & Case #21)

Case #10 is a 51-year-old male patient who has been taking medication for diabetes for 15 years and underwent ALT free flap reconstruction for a defect in his left foot that occurred after orthopedic surgery. From POD 2, the color of the flap gradually turned purplish and showed a congestive appearance. Conservative salvage using heparin gauze was attempted, but the effect was not significant. Subsequently, venous congestion progressed, and the dT of NS-PF value continued to increase. By POD 7, the flap became darker in color and eventually led to total necrosis. The dT of NS-PF was 1.2 on POD 0 and increased to 3.5 by POD 7, indicating significant venous congestion and the resulting necrosis. Case #21 is a 49-year-old female patient with no medical history or medication history who suffered a right distal tibia-fibula fracture after a traffic accident. A peroneal artery perforator-based fasciocutaneous flap was performed to reconstruct a defect exposing the metal plate after reduction with plate fixation for an ankle fracture. From POD 1, the flap began to become hyperemic from the distal portion and progressed with a congestive appearance. Salvage was performed using leech therapy. Until POD 7, a similar appearance was maintained, but thereafter, the central portion showed improvement in congestion, and only partial necrosis of the distal portion remained on POD 14. The dT of NS-PF initially showed an increasing trend, being 1.0 on POD 0 and 2.5 on POD 7, but later decreased to 0 by POD 14, indicating improvement in congestion and partial recovery. (Figure 5).

 doi:10.20944/preprints202406.1185.v1

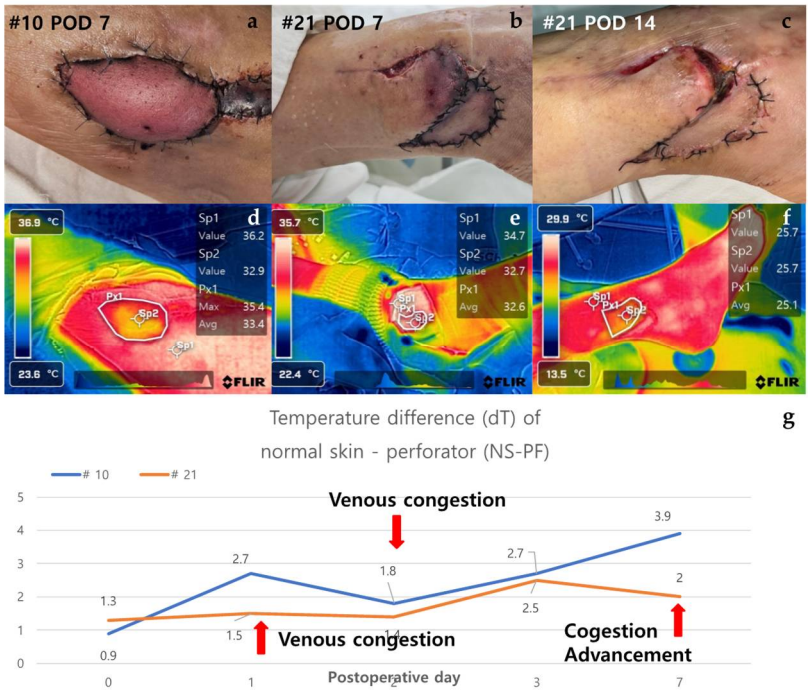

Figure 5. Analysis of cases of venous congestion in necrosis group (#10 & #21). Case #10 is a 51-year-old male patient who underwent ALT reconstruction for an ankle defect that had occurred after orthopedic surgery. The flap showed venous congestion since POD 1, and it gradually worsened. (**a**) On POD 7, the overall color of the flap was purple with edematous change. Case #21 - A 49-year-old female patient underwent peroneal artery perforator based flap for a defect that occurred after orthopedic surgery. Venous congestion in the flap started, with the flap color appearing purple since POD 2, and leech therapy for flap salvage was carried out. (**b**) On POD 7, the distal part of the flap still showed features of congestion, but the central part showed improvement with a lightening of color. (**c**) On POD 14, the necrotic area was demarcated, resulting in distal partial necrosis. (**d**), (**e**) In the thermal images of POD 7, both flaps appeared yellow in color as the temperature dropped. (**f**) In the thermal image of Case #21 on POD 14, the difference in temperature decreased in comparison to POD7. (**g**) The graph showed an upward trend over time from the point of venous congestion, but in Case #21, the temperature difference decreased as the congestion improved. Abbreviations: POD, Post-Operative Day; dT, Temperature Difference; NS-PF, normal skin-perforator; ALT, The anterolateral thigh.

3.2.5. Case in Which a New Flap Was Applied after Salvage Procedure for Arterial Insufficiency (Case #12 & Case #14)

Case #12 is a 48-year-old male patient who underwent a thoracodorsal artery perforator (TDAP) free flap for a defect that occurred after orthopedic surgery due to a fracture of the left distal tibia. On POD 1, doppler sound of the anastomosed vessel could not be heard, and it was judged as arterial occlusion. Despite the salvage procedure, the flap failed, and an ALT free flap was re-applied. The new flap remained stable without necrosis on POD 7. Initially, the dT of NS-PF was 2.0 on POD 0 but increased to 2.8 on POD 1, reflecting the arterial insufficiency. After the application of the new flap, the dT of NS-PF decreased to 0.7 on POD 7, indicating the success of the new flap. Case #14 is a 75-year-old male patient who underwent burr-hole drainage several times due to subdural hemorrhage and was hospitalized due to surgical site infection. ALT free flap was performed for a scalp defect where a plate fixed to the skull after the site of the craniotomy was exposed. On POD 1, the flap was pale in the center and mottled around the margins of the flap, suggesting arterial occlusion. Despite the salvage procedure, the flap failed, and a vastus lateralis muscle free flap was performed. However, the new flap also showed signs of arterial occlusion and progressed to total necrosis. Initially, the dT of NS-PF was 1.8 on POD 0 and increased to 3.0 on POD 1, similar to Case #12. However, after the new flap was applied, the dT of NS-PF further increased to 3.5 on POD 7, indicating continued vascular compromise and eventual total necrosis. The contrasting clinical

 doi:10.20944/preprints202406.1185.v1

courses of the two cases were clearly distinguished by the decrease and increase in the dT of NS-PF values. In Case #12, the successful salvage with a new flap was reflected by a significant decrease in dT of NS-PF, while in Case #14, the failure of the new flap was indicated by the continued increase in dT of NS-PF. (Figure 6).

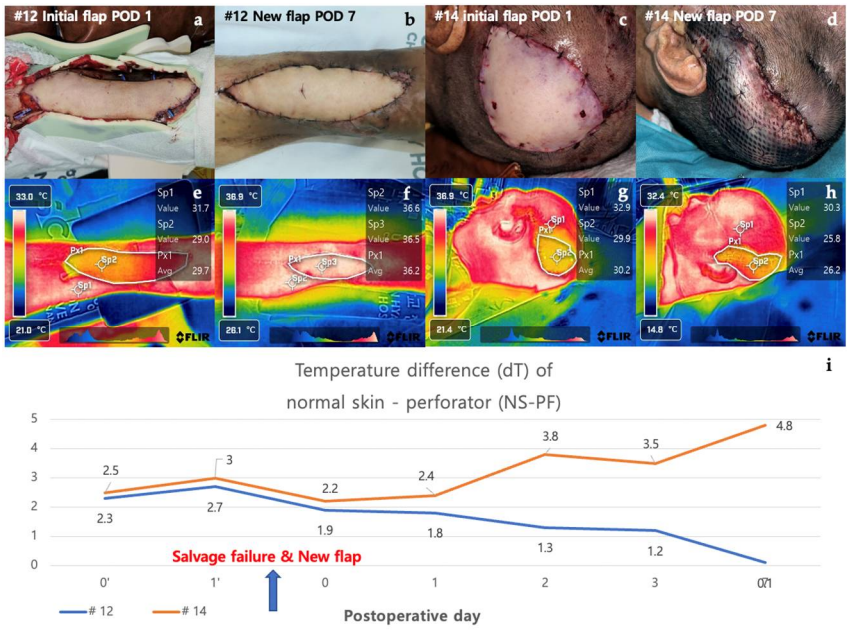

Figure 6. Analysis of cases in which a new flap was applied after salvage procedure for arterial insufficiency (#12 & #14). Case #12 is a 48-year-old male patient who underwent TDAP free flap for a defect occurred after orthopedic surgery due to a fracture of the left distal tibia. (**a**) On POD 1, the color of the flap was pale and mottled, indicating arterial occlusion of the flap. The salvage procedure, re-anastomosis, failed and was covered with a new ALT free flap. (**b**) The new flap remained stable without necrosis on POD 7. Case #14 is a 75-year-old male patient who underwent ALT free flap for a defect caused by a surgical site infection of the scalp. (**c**) As with case #12 on POD 1, the color of the flap was pale and mottled, indicating arterial occlusion of the flap. The salvage procedure in the form of a re-anastomosis failed and was covered with a new vastus lateralis muscle free flap. (**d**) The flap showed signs of arterial occlusion even after reoperation, and it progressed to total necrosis with overall darkening of color. (**e**), (**f**) When there was arterial occlusion, the flap appeared yellow overall, but when the new flap remained stable, it appeared white. (**g**), (**h**) The flap had an overall yellow color on thermal imaging due to arterial occlusion. (**i**) The two graphs showed a pattern of increasing temperature difference as arterial occlusion occurred in the early stages, but showed a contrasting course after the application of a new flap. Abbreviations: POD, Post-Operative Day; dT, Temperature Difference; NS-PF, normal skin-perforator; TDAP free flap, The thoracodorsal artery perforator free flap; ALT free flap, The anterolateral thigh free flap.

3.2.6. The Difference between the Temperature of Perforator Area and the Average Temperature of Total Flap (dT of PF-AFP).

On POD 0, both the necrosis and non-necrotic groups showed positive PF-AFP values, with 0.539 in the non-necrosis group and 0.175 in the necrosis group, showing no significant difference ($p = 0.118$). However, from POD 1 to POD 7, the necrosis group showed positive values while the non-necrosis group showed negative values. This difference was statistically significant (Table 4).

4. Discussion

Skin grafts and flap surgeries are two surgical techniques that are commonly utilized by plastic surgeons when a defect cannot be closed by primary or secondary intention. In plastic surgery, the choice between skin grafts and flap surgeries depends on the type and condition of the wound. These methods have distinct indications and purposes based on their technical differences and the specific needs of the reconstruction. Skin grafts involve transferring a thin layer of skin from a donor site to

 doi:10.20944/preprints202406.1185.v1

a recipient site, which is ideal for superficial defects with good vascular beds. However, they may not be suitable for areas with poor vascularization or deeper tissue loss. In contrast, flap surgeries involve transferring a full thickness of tissue, including skin, muscle, and blood vessels, from one part of the body to another, maintaining its own blood supply. This makes flap surgeries essential for reconstructing defects where blood supply is compromised or where complex three-dimensional tissue reconstruction is needed.

Within flap surgeries, there are two main types: pedicled flaps and free flaps. They represent distinct methods in reconstructive surgery, each with specific applications and characteristics [1]. Pedicled flaps retain their original blood supply through a connected pedicle, making them suitable for shorter distances between the donor and recipient sites and generally reducing the risk of vascular complications. They are favored for their reliability and less demanding microsurgical requirements. Free flaps, on the other hand, involve completely detaching the tissue, including its blood vessels, and microsurgically reconnecting it to blood vessels at the recipient site. This allows for tissue transfer over longer distances and offers greater versatility in tissue types, making them preferable for more complex reconstructions [8,9].

Flap surgery remains the most prevalent and practical surgical approach within the realm of plastic surgery. The demand for flap surgery is on the rise due to several factors, including the increasing incidence of malignant tumors and the growing need for immediate breast reconstruction following mastectomy [10,11]. Extensive research has been conducted on flap surgery, revealing its evolving complexity and the advancements in surgical techniques that continue to enhance its efficacy and outcomes.

The most important factor in flap surgery is flap vascularity, and most flap complications are associated with flap vascular compromise [12]. Vascular compromise is largely divided into two types: arterial occlusion and venous congestion. The pathophysiology of arterial occlusion causes insufficient oxygen delivery and a concomitant deficiency in the elimination of harmful metabolites from the tissues that are impacted. The outcomes include reactive oxygen species (ROS) buildup, an influx of inflammatory cells like neutrophils and macrophages, and a gradual release of cytokines, which creates a cycle of inflammation that eventually results in tissue necrosis [13]. The main variables that link the biochemical pathways between tissue necrosis and prolonged ischemia are reactive oxygen species (ROS), which cause microcirculatory damage that leads to permanent deterioration and harm. When arterial flow is persistent in venous congestion, the intravascular pressure rises and the microvasculature bleeds into the extra-vascular space. The vessels externally compress and collapse as a result of the elevated extravascular pressure. Edema that develops in the interstitial tissue prevents oxygen from diffusing through the tissue, causing more tissue damage [13–15]. The complications of flap surgery involve flap failure, leading to secondary flap surgery, partial or total loss of the flap. For the successful survival of the flap, flap monitoring is essential immediately after surgery, and, if necessary, procedures such as salvage are required.

In reconstructive microsurgery, perforator flaps have become a significant development due to their ability to preserve major vessels and muscle function while allowing less invasive reconstruction. A perforator flap is defined as a flap based on a vessel that perforates the envelope of the target tissue to be transferred. This envelope could be the superficial fascia for skin, the deep fascia for muscle, the periosteum for bone, or the perineurium for nerve. The evolution of perforator flaps has enabled surgeons to perform complex three-dimensional reconstructions with improved outcomes and reduced donor site morbidity. This new definition helps in precisely classifying all flaps, ensuring a better understanding and application in reconstructive procedures [16].

Conventionally, flap monitoring is often performed with subjective methods such as clinical observation of skin color, skin turgor, flap temperature, and capillary refill time. These methods rely on the surgeon's experience and judgment to assess the viability of the flap postoperatively [17]. A normal flap typically exhibits several key criteria. It should feel warm to the touch, indicating good perfusion. The color should be a healthy, pink shade. The capillary refill time should be less than 2 seconds when pressed and released. The flap should have good skin turgor, with rapid return to its original position after being pinched. In some cases, the flap should retain normal sensation, although this can vary depending on the type and location of the flap [18]. When there is an issue with blood flow, specific signs can indicate whether the problem is arterial insufficiency or venous congestion. In the case of arterial insufficiency, the flap may appear pale or white due to insufficient arterial blood

 doi:10.20944/preprints202406.1185.v1

supply. It may feel cool to the touch and exhibit a prolonged capillary refill time, often more than 2 seconds. If not addressed, arterial insufficiency can lead to necrosis, or tissue death. On the other hand, venous congestion typically presents with cyanosis, a blue or dusky appearance due to poor venous outflow. The flap may become swollen and edematous. Despite the congestion, the flap may feel warm and have a delayed capillary refill time, similar to arterial insufficiency but with a bluish color [19]. In addition to these subjective methods, various objective methods utilizing medical devices are also used to monitor flaps. Numerous methods for monitoring flaps have been extensively studied, each presenting distinct advantages and disadvantages shown in Table 5, for example [20–26] (Table 5). However, despite the extensive exploration of monitoring methodologies, there is currently no universally established gold standard among these modalities. Each method has its limitations, such as the requirement for specialized equipment, potential invasiveness, and operator dependency.

Various studies related to infrared thermography for flaps have been conducted for a long time, and interest in this field has recently increased. Many studies, such as burn depth analysis and preoperative perforator mapping, have been conducted, and there are also many existing studies that apply infrared thermography to flap monitoring [27,28]. These studies show a diverse range of methods and results.

In rat models of this study, a model that induces flap necrosis is required. To understand this, it is essential to introduce the concepts of anterograde flaps and reverse flaps. Anterograde flaps have blood flowing in the natural direction, from the center of the body towards the periphery. This configuration typically results in smooth and stable hemodynamics, with minimal vascular resistance, ensuring adequate blood supply and higher survival rates of the flap. In contrast, reverse flaps involve blood flow in the opposite direction, from the distal part of the flap back towards the center. This reversal can increase vascular resistance and potentially lead to less stable blood flow, making the flap more prone to ischemia and necrosis [29–32]. In this study, a caudally based reverse McFarlane flap model was used in rats to intentionally induce flap necrosis for observational purposes. This model is advantageous for studying necrosis because the vascularity of the distal portion of the flap decreases over time, leading to necrosis [33,34]. Thermal imaging was employed to monitor these changes, with temperatures visualized in color gradients (white to blue, indicating decreasing temperatures). Areas undergoing necrosis displayed lower temperatures compared to viable tissue, particularly noticeable on the undersurface of the flap. On POD 3 and POD 7, the average temperature in the necrotic area did not significantly differ from the total flap area, likely due to the influence of core body temperature (Table 1). Since rats have minimal dorsal fat tissue, the skin flap is in direct contact with the body core, which affects the temperature distribution [35]. This core temperature effect minimized the temperature gradient between necrotic and non-necrotic areas, making the impact of external factors more prominent.

In the clinical cases, this study obtained the data by comparing the temperature between normal skin and the perforator of the flap and comparing the temperature of the perforator point of the flap with the average temperature of the entire flap area using infrared thermal imaging in the patients group.

In R. Kraemer's study, they evaluated flap skin temperature and capillary microcirculation through postoperative monitoring using a digital infrared surface thermometer combined with laser-doppler and photospectrometry. They proved their hypothesis that the flap skin temperature decreases when there is arterial thrombosis or venous compromise [36]. The other previous studies demonstrated that if microvascular compromise occurs, the flap surface temperature decreases and temperature difference with adjacent skin increase [37,38]. In the same context as these, the non-necrosis group showed a decreasing trend in the temperature difference between normal skin and perforator (dT of NS-PF) over time, but cases with vascular compromise showed an upward trend in the temperature difference between normal skin and flap due to the flap's temperature dropping further (Figure 7). Although this study did show a statistically significant difference in POD 3 and POD 7, there was no statistically significant difference between the non-necrosis group and the necrosis group until POD 2. However, because early rapid detection of vascular compromise and salvage of the flap is important, it should not be considered as absolute guidance but can be used as a supplementary indicator [39].

 doi:10.20944/preprints202406.1185.v1

In Case #7 and #13, the dT of NS-PF value decreased as time passed compared to the initial stage, but in Case #10 and #21, which showed venous congestion, the temperature of the perforator decreased compared to normal skin as time passed, and the dT of NS-PF value increased. However, in Case #21, the temperature of the perforator increased again from POD 7 as congestion improved through leech therapy, and it ultimately progressed to partial necrosis rather than total necrosis. Therefore, when venous congestion occurs, it indicates that if the dT of NS-PF value does not increase steadily but decreases, the progression to total necrosis may not occur (Figure 5).

Case #12 and Case #14 are cases in which salvage procedures and new flap applications were performed on POD 1 due to arterial occlusion. In both cases, the dT of NS-PF value on POD 1 was higher than the average of the non-necrosis group. In addition, when comparing Case #14 with Case #10, where venous congestion is represented, it can be confirmed that the dT of NS-PF value is higher in Case #14 with arterial insufficiency than in Case #10 with venous congestion. However, after applying a new flap, a contrasting, downwards trend of dT of NS-PF value can be confirmed depending on the presence or absence of flap necrosis (Figure 6).

In Figure 7, the temperature difference between perforator and average of flap (dT of PF-AFP) in the non-necrosis group showed a positive value in all cases from POD 0 to POD 7, except for 1-2 points, while in the necrosis group, it almost always showed a negative value (Figure 8). A positive value of dT of PF-AFP can be interpreted as the temperature of the perforator being higher than the average temperature of the flap, with a negative value meaning the opposite. In the study by Whitaker IS et al., mapping of the deep inferior epigastric artery perforator was carried out using a dynamic infrared thermal camera by performing a cold challenge with a water pack and utilizing the hot spot appearing on the camera to measure the temperature at the perforator with the most abundant flow of heat through the vascular flow of the perforator as the flap re-warmed [40]. The study by Perng CK et al. explained that the surface temperature of the flap was determined by three mechanisms: heat from blood flow entering the flap, heat conduction from tissue located at the bottom of the flap, and heat loss to the air in contact with the flap surface [41]. When applied to this study, if the average temperature of the perforator and the entire area of the flap (which is limited to the inside of the flap) are compared, the other two heat sources are unified, and temperature comparison is possible as heat from blood flow. In addition, since all flaps entered theatre lower than room temperature and thermal imaging was performed 10 minutes later, this can be considered a form of cold challenge. Of course, although the temperature of the perforator site of the flap is not clearly distinguishable from the overall temperature of the flap in terms of color, it is possible to compare the temperature of the perforator and the average temperature of the flap using thermal imaging analysis software. If vascular compromise occurs due to reasons such as thrombosis, malfunction of the circulation inside the flap may occur, and the difference between the temperature of the perforator site and the average temperature of the entire flap may decrease. Therefore, if the dT of PF-AFP value is less than 0, it can be interpreted that there is microvascular compromise in the flap.

Many previous studies analyzed temperature in two methods in flap monitoring using infrared thermography. The first was to measure the absolute temperature gradient of the flap itself, and the other was to measure the gradient in temperature difference between the flap and adjacent normal skin. This study utilized the latter method but showed limitations in early flap monitoring due to variables in temperature measurement of normal skin. Since comparisons cannot be made between flaps on different patients or on different sites, there is a lot of bias towards environmental variables. However, comparing perforator temperature and average temperature within the flap itself can reduce other biases and allow a more accurate evaluation of vascular compromise.

There are several limitations of this study. The sample size, firstly, was too small to evaluate the efficacy of flap monitoring through thermal imaging - Due to the small number of necrosis cases and the inconsistent size or type of flap, it is assumed that the lack of sufficient sample size prevented the derivation of statistical significance. Secondly, we measured the temperature of normal skin at a specific point, but this is somewhat unreliable as it does not represent the temperature of normal skin throughout. For the study by S. Hummelink et al., the mean temperature value within a specific area of adjacent normal skin had been marked and used for comparison instead [37]. In addition, due to the nature of the FLIR camera, various biases are likely to occur due to the influence of the surrounding environment. MA Moran-Romero et al. argued that free flap monitoring through

 doi:10.20944/preprints202406.1185.v1

thermal imaging could produce ambiguous results [42]. However, we compensated for this by conducting temperature measurements in a surgical theatre where temperature and humidity were controlled and there was a unified dress code. Also, upon comparison of the results, we analyzed the gradient of temperature differences as opposed to absolute temperature values.

It is difficult to evaluate the microvascular flow of the flap with absolute value of results obtained through infrared thermal assessment using a FLIR camera. However, the gradient of the temperature difference between normal skin and the perforator over time can be a guide in interpreting the overall course of the flap. In addition, this study suggests a novel method for flap monitoring using infrared thermal imaging with the analysis of the temperature difference between the perforator and the average temperature of the flap, which has sufficient value as a supplementary indicator in judging vascular compromise. Above all, the FLIR camera is a contact-free modality that does not harm the flap, and its high convenience will be more frequently utilized in flap monitoring.

Table 5. Modalities used in flap monitoring.

Monitoring Method	Advantages	Limitations	References
Clinical Examination	Non-invasive Widely available Low cost	Limited applicability in buried flaps Risk of poor interrater agreement due to inconsistent flap (failure) appearances	[20]
Acoustic Doppler Sonography	Non-invasive High sensitivity & specificity Real-time monitoring	Limited applicability in buried flaps Operator-dependent Limited ability to detect venous thrombosis	[20,21]
Implantable Doppler	Continuous monitoring High sensitivity & specificity Real-time monitoring	Invasive Requires surgical implantation Risk of infection Limited applicability in buried flaps	[20,21]
Indocyanine Green Fluorescence Angiography	Non-invasive High sensitivity & specificity Real-time monitoring Ability to detect venous thrombosis	Limited applicability in buried flaps Requires specialized equipment Limited ability to detect arterial thrombosis	[20,23]
Near-Infrared Spectroscopy	Non-invasive Real-time monitoring Ability to detect arterial thrombosis	Limited applicability in buried flaps Requires specialized equipment Limited ability to detect venous thrombosis	[22]
Tissue Oximetry	Non-invasive Real-time monitoring Ability to detect arterial thrombosis	Limited applicability in buried flaps Requires specialized equipment Limited ability to detect venous thrombosis	[24]
Transcutaneous Oximetry measurement	Non-invasive Quantifying measurement Potential for thermal injury	Limited applicability in buried flaps Time required for measurement Low sensitivity	[25,26]

 doi:10.20944/preprints202406.1185.v1

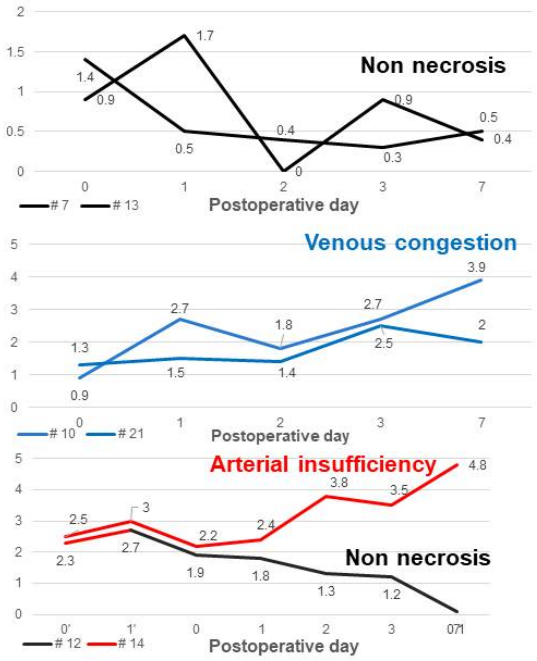

Figure 7. The graph of the temperature difference between normal skin and perforator according to clinical course of the flaps. The black graph, which represents the non-necrosis group, shows a downward trend in values over time. The red graph represents the group with arterial insufficiency, and the blue graph represents the group with venous congestion. Both red and blue show an upward trend in values over time.

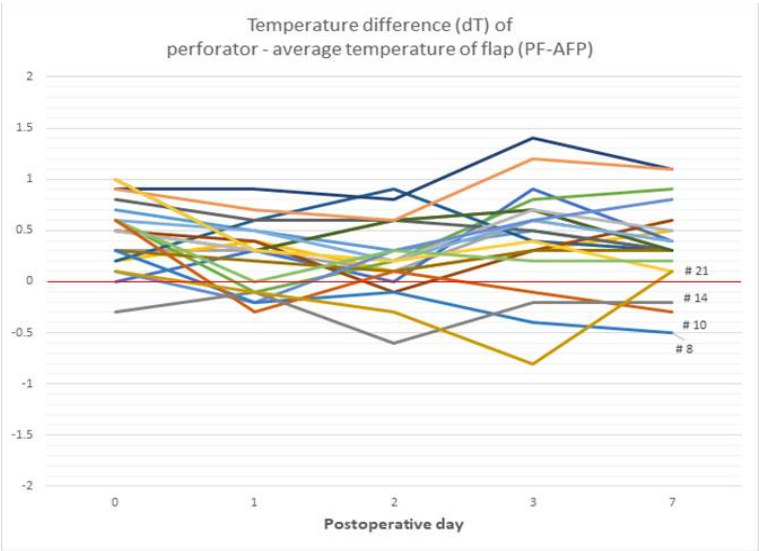

Figure 8. The graph of the temperature difference between perforator and mean temperature of flap. The temperature difference between perforator and average of flap (dT of PF-AFP) in the non-necrosis group showed a positive value in all cases from POD 0 to POD 7, except for 1-2 points, while in the necrosis group, it almost always showed a negative value.

5. Conclusions

Numerous studies are investigating flap monitoring using infrared thermal imaging. FLIR cameras offer the benefits of being non-invasive and highly convenient. While further research is necessary before FLIR cameras can serve as definitive indicators for vascular compromise during flap monitoring, they can effectively function as auxiliary tools for assessing and predicting the overall clinical progression of flaps. This study introduces a novel method for flap monitoring via infrared

 doi:10.20944/preprints202406.1185.v1

thermography by analyzing the temperature differential between the perforator area and the average flap temperature, demonstrating significant potential for enhancing the flap monitoring process.

Author Contributions: Conceptualization, Hyun Kim, M.D, Si Hyun Kwak, M.D. and Hwan Jun Choi, M.D. Ph.D.; methodology, Si Hyun Kwak, M.D., Jun Hyuk Kim, M.D. Ph.D. and Hwan Jun Choi, M.D. Ph.D.; software, Hyun Kim, M.D, Si Hyun Kwak, M.D., Je Youn Byeon, M.D. and Da Woon Lee, M.D. Ph.D.; validation, Jun Hyuk Kim, M.D. Ph.D. and Hwan Jun Choi, M.D. Ph.D.; formal analysis, Si Hyun Kwak, M.D.; investigation, Da Woon Lee, M.D. Ph.D., Jun Hyuk Kim, M.D. Ph.D. and Hwan Jun Choi, M.D. Ph.D.; resources, Je Youn Byeon, M.D., Da Woon Lee, M.D. Ph.D., Jun Hyuk Kim, M.D. Ph.D. and Hwan Jun Choi, M.D. Ph.D.; data curation, Hyun Kim, M.D, Si Hyun Kwak, M.D., Soomin Lim and Hwan Jun Choi, M.D. Ph.D.; writing—original draft preparation, Hyun Kim, M.D, Si Hyun Kwak, M.D. and Soomin Lim; writing—review and editing, Hyun Kim, M.D. and Hwan Jun Choi, M.D. Ph.D.; visualization, Hyun Kim, M.D. and Si Hyun Kwak, M.D.; supervision, Hwan Jun Choi, M.D. Ph.D.; project administration, Jun Hyuk Kim, M.D. Ph.D.; funding acquisition, Hwan Jun Choi, M.D. Ph.D. All authors have read and agreed to the published version of the manuscript.

Institutional Review Board Statement: The study was conducted in accordance with the Declaration of Helsinki, and approved by the Institutional Review Board of. Soonchunhyang University Cheonan Hospital (IRB number: 2023-12-071).” for studies involving humans. OR “The animal study protocol was approved by the Institutional Animal Care and Use Committee (IACUC) of Soonchunhyang University (Approval number: SCH-0062).

Informed Consent Statement: Informed consent was obtained from all subjects involved in the study.

Acknowledgments: This work was supported by the National Research Foundation of Korea (NRF) grant funded by the Korea government (MSIT) (2020R1A2C1100891), and was supported by Soonchunhyang University research fund.

Conflicts of Interest: The authors declare no conflicts of interest.

References

1. Gottlieb, L. J., & Krieger, L. M. (1994). From the reconstructive ladder to the reconstructive elevator. Plastic and Reconstructive Surgery, 93(7), 1503-1504.
2. Shen, A. Y., Lonie, S., Lim, K., Farthing, H., Hunter-Smith, D. J., & Rozen, W. M. (2021). Free flap monitoring, salvage, and failure timing: A systematic review. Journal of Reconstructive Microsurgery, 37(3), 300-308.
3. Knoedler, S., Hoch, C. C., Huelsboemer, L., Knoedler, L., Stögner, V. A., Pomahac, B., Kauke-Navarro, M., & Colen, D. (2023). Postoperative free flap monitoring in reconstructive surgery-man or machine? Frontiers in Surgery, 10, 1130566.
4. Hosein, R. C., Cornejo, A., & Wang, H. T. (2016). Postoperative monitoring of free flap reconstruction: A comparison of external Doppler ultrasonography and the implantable Doppler probe. Plastic Surgery (Oakville), 24(1), 11-19.
5. Rabbani, M. J., Bhatti, A. Z., & Shahzad, A. (2021). Flap monitoring using thermal imaging camera: A contactless method. Journal of the College of Physicians and Surgeons Pakistan, 30(6), 703-706.
6. John, H. E., Niumsawatt, V., Rozen, W. M., & Whitaker, I. S. (2016). Clinical applications of dynamic infrared thermography in plastic surgery: A systematic review. Gland Surgery, 5(2), 122-132.
7. Hennessy, O., & Potter, S. M. (2019). Use of infrared thermography for the assessment of free flap perforators in autologous breast reconstruction: A systematic review. JPRAS Open, 23, 60-70.
8. Sittitrai, P., Ruenmarkkaew, D., & Klibngern, H. (2022). Pedicled flaps versus free flaps for oral cavity cancer reconstruction: A comparison of complications, hospital costs, and functional outcomes. International Archives of Otorhinolaryngology, 27(1), e32-e42.
9. Neusner, A. D., Pribaz, J. J., & Guo, L. (2022). Free your mind, not your flap. Plastic and Reconstructive Surgery - Global Open, 10(6), e4384.
10. Lewis, R. S., & Kontos, M. (2009). Autologous tissue immediate breast reconstruction: Desired but oncologically safe? International Journal of Clinical Practice, 63(11), 1642-1646.
11. Suh, J. M., Chung, C. H., & Chang, Y. J. (2021). Head and neck reconstruction using free flaps: A 30-year medical record review. Archives of Craniofacial Surgery, 22(1), 38-44.
12. Khouri, R. K., & Shaw, W. W. (1992). Monitoring of free flaps with surface-temperature recordings: Is it reliable? Plastic and Reconstructive Surgery, 89(3), 495-499.
13. Nguyen, G. K., Hwang, B. H., Zhang, Y., Monahan, J. F., Davis, G. B., Lee, Y. S., Ragina, N. P., Wang, C., Zhou, Z. Y., Hong, Y. K., Spivak, R. M., & Wong, A. K. (2013). Novel biomarkers of arterial and venous ischemia in microvascular flaps. PLoS One, 8(8), e71628.

 doi:10.20944/preprints202406.1185.v1

14. Amon, M., Menger, M. D., & Vollmar, B. (2003). Heme oxygenase and nitric oxide synthase mediate cooling-associated protection against TNF-alpha-induced microcirculatory dysfunction and apoptotic cell death. FASEB Journal, 17(2), 175-185.
15. Menger, M. D., Rücker, M., & Vollmar, B. (1997). Capillary dysfunction in striated muscle ischemia/reperfusion: On the mechanisms of capillary "no-reflow". Shock, 8(1), 2-7.
16. Akita, S. (2020). Advances and challenges in perforator flap surgery. Global Health & Medicine, 2(1), 114-121. https://doi.org/10.35772/ghm.2020.01058
17. Shen, A. Y., Lonie, S., Lim, K., Farthing, H., Hunter-Smith, D. J., & Rozen, W. M. (2021). Free flap monitoring, salvage, and failure timing: A systematic review. Journal of Reconstructive Microsurgery, 37(3), 300-308.
18. Chao, A. H., Meyerson, J., Povoski, S. P., & Kocak, E. (2013). A review of devices used in the monitoring of microvascular free tissue transfers. Expert Review of Medical Devices, 10(5), 649-660.
19. Nguyen, G. K., Hwang, B. H., Zhang, Y., Monahan, J. F., Davis, G. B., Lee, Y. S., ... & Wong, A. K. (2013). Novel biomarkers of arterial and venous ischemia in microvascular flaps. PLoS One, 8(8), e71628.
20. Lohman, R. F., Langevin, C. J., Bozkurt, M., Kundu, N., & Djohan, R. (2013). A prospective analysis of free flap monitoring techniques: Physical examination, external Doppler, implantable Doppler, and tissue oximetry. Journal of Reconstructive Microsurgery, 29(1), 51-56.
21. Chao, A. H., Meyerson, J., Povoski, S. P., & Kocak, E. (2013). A review of devices used in the monitoring of microvascular free tissue transfers. Expert Review of Medical Devices, 10(5), 649-660.
22. Chen, Y., Shen, Z., Shao, Z., & Yu, P. (2016). Free flap monitoring using near-infrared spectroscopy: A systemic review. Annals of Plastic Surgery, 76(5), 590-597.
23. Ricci, J. A., Vargas, C. R., Lin, S. J., Tobias, A. M., Taghinia, A. H., & Lee, B. T. (2016). A novel free flap monitoring system using tissue oximetry with text message alerts. Journal of Reconstructive Microsurgery, 32(5), 415-420.
24. Wang, Z., Jiao, L., Chen, S., Li, Z., Xiao, Y., Du, F., Huang, J., & Long, X. (2023). Flap perfusion assessment with indocyanine green angiography in deep inferior epigastric perforator flap breast reconstruction: A systematic review and meta-analysis. Microsurgery, 43(6), 627-638.
25. Lee, D. W., Hwang, Y. S., Byeon, J. Y., Kim, J. H., & Choi, H. J. (2023). Does the advantage of transcutaneous oximetry measurements in diabetic foot ulcer apply equally to free flap reconstruction? World Journal of Clinical Cases, 11(31), 7570-7582.
26. Nam, H. J., Wee, S. Y., Kim, S. Y., Jeong, H. G., Lee, D. W., Byeon, J. Y., Park, S. H., & Choi, H. J. (2023). The correlation between transcutaneous oxygen pressure (TcPO2) and forward-looking infrared (FLIR) thermography in the evaluation of lower extremity perfusion according to angiosome. International Wound Journal. https://doi.org/10.1111/iwj.14431
27. Asif, A., Poyiatzis, C., & Raheman, F. J. (2022). The use of infrared thermography (IRT) in burns depth assessment: A diagnostic accuracy meta-analysis. European Burn Journal, 3(3), 432-446.
28. Berner, J. E., Pereira, N., Troisi, L., Will, P., Nanchahal, J., & Jain, A. (2021). Accuracy of infrared thermography for perforator mapping: A systematic review and meta-analysis of diagnostic studies. Journal of Plastic, Reconstructive & Aesthetic Surgery, 74(6), 1173-1179.
29. Park, C. (2021). Applications of the reverse McFarlane flap in hand surgery. Journal of Hand Surgery, 46(5), 432-439.
30. Lee, Y. S., & Kim, S. H. (2022). Reconstructive techniques using reverse McFarlane flaps. Plastic and Reconstructive Surgery, 49(3), 210-215.
31. Patel, R., & Tan, E. (2020). Vascular considerations in reverse McFarlane flap procedures. International Journal of Reconstructive Surgery, 36(2), 95-102.
32. Nguyen, A., & Patel, V. (2022). Retrograde flap hemodynamics and clinical applications. Journal of Microsurgery, 39(5), 315-320.
33. Sowa, M. G., Friesen, J. R., Levasseur, M., Schattka, B., Sigurdson, L., & Hayakawa, T. (2012). The utility of near infrared imaging in intra-operative prediction of flap outcome: A reverse McFarlane skin flap model study. Journal of Near Infrared Spectroscopy, 20(5), 601-615.
34. Ibne Mahbub, M. S., Kim, Y. J., Choi, H., & Lee, B. T. (2023). Papaverine loaded injectable and thermosensitive hydrogel system for improving survival of rat dorsal skin flaps. Journal of Materials Science: Materials in Medicine, 34(6), 28.
35. Czapla, N., Lokaj, M., Falkowski, A., & Prowans, P. (2014). The use of thermography to design tissue flaps - experimental studies on animals. Videosurgery and Other Miniinvasive Techniques, 9(3), 319-328.
36. Kraemer, R., Lorenzen, J., Knobloch, K., Papst, S., Kabbani, M., Koennecker, S., & Vogt, P. M. (2011). Free flap microcirculatory monitoring correlates to free flap temperature assessment. Journal of Plastic, Reconstructive & Aesthetic Surgery, 64(10), 1353-1358.

 doi:10.20944/preprints202406.1185.v1

37. Hummelink, S., Kruit, A. S., van Vlaenderen, A. R. W., & et al. (2020). Post-operative monitoring of free flaps using a low-cost thermal camera: A pilot study. European Journal of Plastic Surgery, 43, 589-596.
38. Papillion, P., Wong, L., Waldrop, J., Sargent, L., Brzezienski, M., Kennedy, W., & Rehm, J. (2009). Infrared surface temperature monitoring in the postoperative management of free tissue transfers. Canadian Journal of Plastic Surgery, 17(3), 97-101.
39. Shen, A. Y., Lonie, S., Lim, K., Farthing, H., Hunter-Smith, D. J., & Rozen, W. M. (2021). Free flap monitoring, salvage, and failure timing: A systematic review. Journal of Reconstructive Microsurgery, 37(3), 300-308.
40. Whitaker, I. S., Lie, K. H., Rozen, W. M., & et al. (2012). Dynamic infrared thermography for the preoperative planning of microsurgical breast reconstruction: A comparison with CTA. Journal of Plastic, Reconstructive & Aesthetic Surgery, 65(1), 130-132.
41. Perng, C. K., Ma, H., Chiu, Y. J., Lin, P. H., & Tsai, C. H. (2018). Detection of free flap pedicle thrombosis by infrared surface temperature imaging. Journal of Surgical Research, 229, 169-176.
42. Moran-Romero, M. A., & Lopez-Mendoza, F. J. (2022). Postoperative monitoring of free flaps using smartphone thermal imaging may lead to ambiguous results: Three case reports. International Microsurgery, 6(1), 4.